

Feature Article

Anticancer activity studies of ruthenium(II) polypyridyl complexes against human gastric carcinoma SGC-7901 cell



Chuan-Chuan Zeng^a, Cheng Zhang^a, Shang-Hai Lai^a, Hui Yin^{b,*}, Bing Tang^a, Dan Wan^a, Yun-Jun Liu^{a,*}

^a School of Pharmacy, Guangdong Pharmaceutical University, Guangzhou 510006, China

^b Department of Microbiology and Immunology, Guangdong Pharmaceutical University, Guangzhou 510006, China

ARTICLE INFO

Article history:

Received 21 May 2016

Received in revised form 18 June 2016

Accepted 23 June 2016

Available online 25 June 2016

Keywords:

Ruthenium(II) polypyridyl complex

Apoptosis

Cell invasion

ROS

Western blot analysis

ABSTRACT

A new ligand TCPI and its three ruthenium(II) polypyridyl complexes [Ru(N-N)₂(TCPI)](PF₆)₂ (N-N = bpy: 2,2'-bipyridine **1**; phen: phenanthroline **2**; dmp: 2,9-dimethyl-1,10-phenanthroline **3**) were synthesized and characterized by elemental analysis, ESI-MS, ¹H NMR, IR, absorption and emission spectra. The cytotoxic activity in vitro of the ligand and complexes against cancer cells SGC-7901, PC-12, HepG-2, SiHa, Eca-109, HeLa and normal cell LO2 was evaluated by MTT method. Complex **3** shows the highest cytotoxic activity toward SGC-7901 cell among the complexes. Interestingly, the complexes show low or no cytotoxic activity against normal cell LO2. The apoptosis in SGC-7901 cell was investigated with AO/EB staining method. The ROS levels and the changes of mitochondrial membrane potential were studied under fluorescent microscope and flow cytometry. The cell invasion, cell cycle arrest and the expression of Bcl-2 family proteins were studied in detail. The results demonstrate that the complexes induce apoptosis in SGC-7901 cell through a ROS-mediated mitochondrial dysfunction pathway, which was accompanied by the regulation of Bcl-2 family proteins.

© 2016 Elsevier B.V. All rights reserved.

Contents

1.	Introduction	211
2.	Experimental	211
2.1.	Materials and method.	211
2.2.	Synthesis of ligand and complexes	212
2.2.1.	Synthesis of ligand TCPI.	212
2.2.2.	Synthesis of [Ru(bpy) ₂ (TCPI)](PF ₆) ₂ (1)	212
2.2.3.	Synthesis of [Ru(phen) ₂ (TCPI)](PF ₆) ₂ (2)	212
2.2.4.	Synthesis of [Ru(dmp) ₂ (TCPI)](PF ₆) ₂ (3)	212
2.3.	Cytotoxicity in vitro.	212
2.4.	Apoptosis assay by AO/EB staining method	212
2.5.	The percentage of apoptotic cells determination by flow cytometry	213
2.6.	Reactive oxygen species (ROS) detection	213
2.7.	Mitochondrial membrane potential assay	213
2.8.	Cell cycle arrest by flow cytometry	214
2.9.	Anti-metastasis study	214
2.10.	Western blot analysis	214
3.	Results and discussion	215
3.1.	Synthesis and characterization	215
3.2.	Cytotoxic activity in vitro	215
3.3.	Apoptosis assay by AO/EB staining method	216
3.4.	Reactive oxygen species (ROS) detection	216
3.5.	Mitochondrial membrane potential assay	216
3.6.	Cell cycle arrest by flow cytometry	217
3.7.	Anti-metastasis studies	217

* Corresponding authors.

E-mail addresses: huiyin0103@163.com (H. Yin), lyjche@163.com (Y.-J. Liu).

3.8. Western blot analysis	218
4. Conclusions	218
Acknowledgments	218
Appendix A. Supplementary material	218
References	218

1. Introduction

Cisplatin was the first metal-based complex, and has been widely used to the treatment of ovarian and testicular cancers [1,2]. The major drawbacks including severe side effects and drug resistance have limited the clinical applications of cisplatin [3–5]. In order to overcome the side effects in platinum-based anticancer drugs, drugs based on other transition metals have been paid more attention [6]. In the search for more effective and selective potential anticancer metallodrugs [7], ruthenium complexes have been considered as potential candidates [8–12]. So far, three typical Ru(III) complexes have succeeded in entering the human clinical trial: NAMI-A (trans-[tetrachlorido(1*H*-imidazole)(dimethyl sulfoxide)] ruthenate(III)), KP1019 (indazolium trans-[tetrachloridobis(1*H*-imidazole) ruthenate(III)]), and KP1339 (sodium trans-[tetrachloridobis(1*H*-imidazole) ruthenate(III)]) [13–18]. NAMI-A and KP1339 have entered into the phase II clinical trial [19]. In recent years, the anticancer activity of ruthenium(II) polypyridyl complexes has attracted great interest, and a number of ruthenium(II) polypyridyl complexes show unique bioactivity. [Ru(dmp)₂(pddppn)]²⁺ (pddppn = phenanthro[1,2-*b*]-1,4-diazabenzodipyrido[3,2-*a*:2',3'-*c*]phenazine) shows high effect on the inhibition of the cell growth against BEL-7402, HeLa, MG-63 and A549 cells with low IC₅₀ values of 1.6 ± 0.4, 9.0 ± 0.8, 1.5 ± 0.2 and 1.5 ± 0.3 μM, respectively [20]. [Ru(phpy)(bpy)(dppn)]⁺ (bpy = 2,2'-bipyridine, dppn = benzo[*i*]dipyrido[3,2-*a*:2',3'-*c*]phenazine) is 6 times more active than the platinum drug against HeLa cells, and it is able to disrupt the mitochondria membrane potential [21]. The complex [Ru(bpy)(phpy)(dppz)]⁺ (phpy = 2-phenylpyridine, dppz = dipyrdo[3,2-*a*:2',3'-*c*]phenazine) was found to be rapidly taken up by cancer cells, and nearly 90% of the complex accumulated in the nuclei of cancer cells after a 2 h incubation [22]. The Ru(II) polypyridyl complex [Ru(bpy)₂(dppn)]Cl₂ (dppn = benzo[*i*]dipyrido[3,2-*a*:2',3'-*c*]phenazine) exhibits high cytotoxicity against two cancer cell lines at low micromolar IC₅₀ values [23].

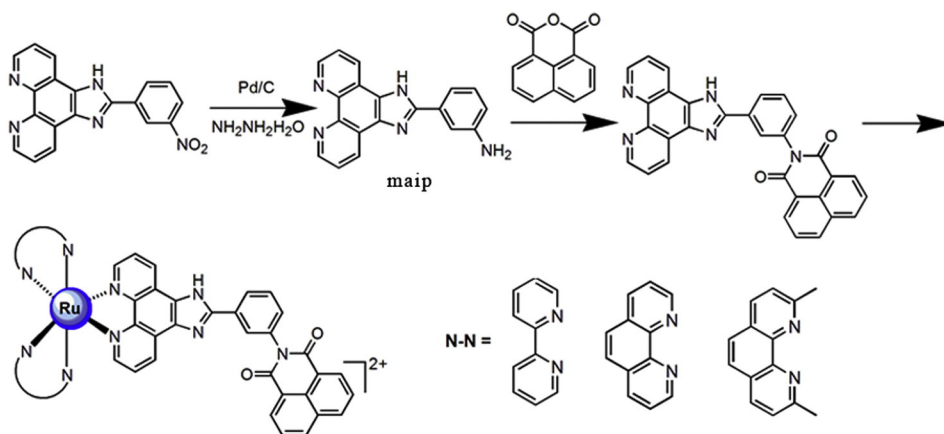
The DNA-binding behaviors show that ruthenium(II) polypyridyl complexes display large DNA-binding affinities and DNA is considered as a main interaction target in the past decades. However, many recent studies revealed that mitochondria act as another vital target [24–30]. To obtain more insight into anticancer activity and further understand

the apoptotic mechanism of ruthenium(II) complexes, in this paper, we synthesized and characterized a new ligand TCPI (TCPI = 2-(3-(1*H*-1,3,7,8-tetraazacyclo-penta[*l*]phenanthren-2-yl)phenyl)benzo[*de*]isoquinoline-1,3-dione) and its three ruthenium(II) polypyridyl complexes [Ru(N-N)₂(TCPI)](PF₆)₂ (N-N = bpy: 2,2'-bipyridine **1**; phen: phenanthroline **2**; dmp: 2,9-dimethyl-1,10-phenanthroline **3**, Scheme 1) by elemental analysis, ¹H NMR and ESI-MS, IR, absorption and emission spectra. The cytotoxicity in vitro of the ligand and complexes against SGC-7901, PC-12, HepG-2, SiHa, Eca-109, HeLa, and normal cell LO2 was evaluated by MTT method. The apoptosis of SGC-7901 cells induced by the complexes was studied under fluorescence microscope and flow cytometry with AO/EB and Annexin V/PI staining method, respectively. The cell cycle arrest of SGC-7901 cells was analyzed by flow cytometry. The reactive oxygen species and mitochondrial membrane potential were also investigated under fluorescence microscope. Additionally, the Matrigel invasion assay was used to determine the effect of the complexes on inhibiting the invasion of SGC-7901 cells. To further explore the apoptotic-inducing mechanism, the expression of the related apoptotic proteins including caspase-3, procaspase-7, Bcl-x, Bcl-2, Bid and Bak was assayed by Western blot.

2. Experimental

2.1. Materials and method

The reagents and solvents we used in the experiments were purchased commercially and used without further purification unless special explanation. Ultrapure Milli-Q water was used in all experiments. DMSO and RPMI 1640 (Roswell Park Memorial Institute) were purchased from GIBCO. RuCl₃·3H₂O was purchased from the Kunming Institution of Precious Metals. 1,10-Phenanthroline was obtained from the Guangzhou Chemical Reagent Factory. Cell lines of SGC-7901 (human gastric carcinoma cell), PC-12 (Sewer rat adrenal pheochromocytoma), HepG-2 (Human hepatocellular carcinoma), SiHa (human cervical squamous cell carcinoma), Eca-109 (esophageal cancer cell line), HeLa (human cervical cancer cell line) and normal cell LO2 were purchased from the American Type Culture Collection. All the cells were cultured in RPMI 1640 supplemented with 10% fetal bovine serum



Scheme 1. The synthetic route of ligand and complexes.

(FBS), penicillin (100 U/mL), and streptomycin (100 µg/mL) and incubated at 37 °C in a 5% CO₂ incubator.

Microanalyses (C, H, and N) were investigated with a Perkin-Elmer 240Q elemental analyzer. Electrospray ionization mass spectra (ESI-MS) were recorded on a LCQ system (Finnigan MAT, USA) using acetonitrile as mobile phase. The spray voltage, tube lens offset, capillary voltage, and capillary temperature were set at 4.50 kV, 30.00 V, 23.00 V, and 200 °C, respectively, and the quoted *m/z* values are for the major peaks in the isotope distribution. ¹H NMR spectra were recorded on a Varian-500 spectrometer with DMSO-*d*₆ as solvent and tetramethylsilane as an internal standard at 500 MHz at room temperature.

2.2. Synthesis of ligand and complexes

2.2.1. Synthesis of ligand TCPI

2-(3-Aminophenyl)imidazo[4,5-*f*] [1, 10]phenanthroline (0.467 g, 1.5 mmol) [31] and 1,8-naphthalic anhydride (0.297 g, 1.5 mmol) were dissolved in 50 mL of DMF and refluxed at 135 °C for 24 h. The cooled solution was filtered, and a yellow precipitate was obtained. Yield: 58%. Anal. calcd for C₃₁H₁₇N₅O₂: C, 75.75; H, 3.49; N, 14.25%. Found: C, 75.72; H, 3.53; N, 14.28%. IR (KBr, cm⁻¹): 3543.5, 3066.3, 2886.1, 2822.0, 1704.9, 1662.8, 1621.3, 1585.9, 1512.4, 1434.7, 1374.2, 1353.9, 1237.2, 1190.7, 802.7, 777.4, 741.3. ESI-MS (DMSO): *m/z* 492 [M + H].

2.2.2. Synthesis of [Ru(bpy)₂(TCPI)](PF₆)₂ (1)

A mixture of cis-[Ru(bpy)₂Cl₂]₂H₂O [32] (0.26 g, 0.50 mmol) and TCPI (0.246 g, 0.5 mmol) in ethanol (50 mL) was refluxed under argon for 8 h to give a clear red solution. Upon cooling, a yellowish brown precipitate was obtained by dropwise addition of saturated aqueous NH₄PF₆ solution. The crude product was purified by column chromatography on neutral alumina with a mixture of CH₃CN–toluene (1:1, v/v) as eluent. The red band was collected. The solvent was removed under reduced pressure and a red powder was obtained. Yield: 72%. Anal. calcd for C₅₁H₃₃N₉F₁₂O₂F₂P₂Ru: C, 51.21; H, 2.78; N, 10.55%. Found: C, 51.16; H, 2.74; N, 10.60%. ¹H NMR (DMSO-*d*₆): δ 9.07 (d, 2H, *J* = 8.5 Hz), 8.87 (d, 2H, *J* = 8.5 Hz), 8.83 (d, 2H, *J* = 8.5 Hz), 8.57 (d, 4H, *J* = 6.0 Hz), 8.42 (d, 1H, *J* = 8.0 Hz), 8.33 (d, 1H, *J* = 6.0 Hz), 8.21 (t, 2H, *J* = 7.0 Hz), 8.12 (t, 2H, *J* = 6.5 Hz), 8.06 (d, 2H, *J* = 5.0 Hz), 7.96 (d, 4H, *J* = 7.5 Hz), 7.84 (d, 3H, *J* = 5.0 Hz), 7.63 (d, 3H, *J* = 5.0 Hz), 7.57 (t, 2H, *J* = 6.0 Hz), 7.35 (t, 2H, *J* = 6.0 Hz). IR (KBr, cm⁻¹): 3627.2, 3071.3, 2883.1, 1708.0, 1666.1, 1603.7, 1585.6, 1512.8, 1465.8, 1446.4, 1355.8, 1315.8, 1272.8, 1238.9, 1198.5, 842.5, 765.8, 557.8. ESI-MS (CH₃CN): *m/z* 1050.2 ([M–PF₆]⁺), 904.4 ([M–2PF₆–H]⁺), 452.8 ([M–2PF₆]²⁺).

2.2.3. Synthesis of [Ru(phen)₂(TCPI)](PF₆)₂ (2)

This complex was synthesized in a manner identical to that described for **1**, with [Ru(phen)₂Cl₂]₂H₂O [32] in place of [Ru(bpy)₂Cl₂]₂H₂O. Yield: 75%. Anal. calcd for C₅₅H₃₃N₉F₁₂O₈P₂Ru: C, 53.09; H, 2.62; N, 10.14%. Found: C, 53.15; H, 2.71; N, 10.19%. ¹H NMR (DMSO-*d*₆): δ 9.06 (d, 2H, *J* = 7.5 Hz), 8.76 (d, 4H, *J* = 5.5 Hz), 8.53 (d, 3H, *J* = 6.5 Hz), 8.48 (d, 2H, *J* = 8.5 Hz), 8.41 (s, 4H), 8.34 (d, 1H), 8.13 (d, 2H, *J* = 5.0 Hz), 8.06 (d, 2H, *J* = 5.0 Hz), 8.01 (d, 2H, *J* = 5.0 Hz), 7.95 (t, 2H, *J* = 7.5 Hz), 7.78–7.74 (m, 6H), 7.67 (d, 2H, *J* =

7.0 Hz). IR (KBr, cm⁻¹): 3495.5, 3064.9, 2928.8, 1708.5, 1603.1, 1584.9, 1512.2, 1461.2, 1428.4, 1355.2, 1238.4, 1199.2, 843.3, 720.8, 557.4. ESI-MS (CH₃CN): *m/z* 1098.0 ([M–PF₆]⁺), 952.4 ([M–2PF₆–H]⁺), 476.9 ([M–2PF₆]²⁺).

2.2.4. Synthesis of [Ru(dmp)₂(TCPI)](PF₆)₂ (3)

This complex was synthesized in a manner identical to that described for **1**, with [Ru(dmp)₂Cl₂]₂H₂O [33] in place of [Ru(bpy)₂Cl₂]₂H₂O. Yield: 67%. Anal. calcd for C₅₉H₄₁N₉F₁₂O₈P₂Ru: C, 54.50; H, 3.18; N, 9.70%. Found: C, 54.44; H, 3.25; N, 9.76%. ¹H NMR (DMSO-*d*₆): δ 8.91 (d, 2H, *J* = 8.5 Hz), 8.85 (d, 2H, *J* = 8.0 Hz), 8.55 (t, 4H, *J* = 6.0 Hz), 8.43 (dd, 4H, *J* = 8.5, *J* = 8.0 Hz), 8.32 (d, 1H, *J* = 8.0 Hz), 8.24 (d, 3H, *J* = 9.0 Hz), 7.95 (dd, 4H, *J* = 8.5, *J* = 7.5 Hz), 7.80 (t, 1H, *J* = 7.5 Hz), 7.62 (d, 1H, *J* = 8.0 Hz), 7.50 (s, 2H), 7.38 (d, 4H, *J* = 5.5 Hz), 1.93 (s, 6H), 1.70 (s, 6H). IR (KBr, cm⁻¹): 3645.8, 3066.3, 2892.9, 1708.6, 1665.8, 1625.9, 1586.2, 1510.3, 1437.0, 1373.9, 1353.6, 1238.3, 1197.5, 842.3, 780.1, 557.2. ESI-MS (CH₃CN): *m/z* 1008.4 ([M–2PF₆–H]⁺), 504.9 ([M–2PF₆]²⁺).

2.3. Cytotoxicity in vitro

3-(4,5-Dimethylthiazole)-2,5-diphenyltetraazolium bromide (MTT) assay procedures were used [34]. Cells were placed in 96-well microassay culture plates (8 × 10³ cells per well) and grown overnight at 37 °C in a 5% CO₂ incubator. Complexes tested were then added to the wells to achieve final concentrations ranging from 10⁶ to 10⁴ M. Control wells were prepared by addition of culture medium (100 mL). The plates were incubated at 37 °C in a 5% CO₂ incubator for 48 h. Upon completion of the incubation, stock MTT dye solution (20 mL, 5 mg/mL) was added to each well. After 4 h, buffer (100 mL) containing dimethylformamide (50%) and sodium dodecyl sulfate (20%) was added to solubilize the MTT formazan. The optical density of each well was measured with a microplate spectrophotometer at a wavelength of 490 nm. The IC₅₀ values were determined by plotting the percentage of cell viability versus concentration on a logarithmic graph and reading off the concentration at which 50% of cells remain viable relative to the control. Each experiment was repeated at least three times to obtain the mean values.

2.4. Apoptosis assay by AO/EB staining method

SGC-7901 cells were seeded onto chamber slides in six-well plates at a density of 2 × 10⁵ cells per well and incubated for 24 h. The cells were cultured in RPMI 1640 supplemented with 10% of fetal bovine serum (FBS) and incubated at 37 °C in 5% CO₂. The medium was removed and replaced with medium (final DMSO concentration, 0.05% v/v) containing the complexes **1**, **2**, and **3** (6.25 µM) for 24 h. The medium was removed again, and the cells were washed with ice-cold phosphate buffer saline (PBS), and fixed with formalin (4%, w/v). Cell nuclei were counterstained with acridine orange (AO) and ethidium bromide (EB) (AO: 100 mg/mL, EB: 100 mg/mL) for 10 min. The cells were observed and imaged with a fluorescence microscope (Nikon, Yokohama, Japan) with excitation at 350 nm and emission at 460 nm.

Table 1

The IC₅₀ (µM) values of ligand and complexes toward selected cell lines.

Comp	SGC-7901	PC-12	HepG-2	SiHa	Eca-109	HeLa	LO2
TCPI	28.8 ± 2.8	14.5 ± 2.4	>200	>200	>200	>200	96.8 ± 3.8
1	18.3 ± 2.2	33.8 ± 1.4	90.8 ± 4.5	39.7 ± 6.6	74.2 ± 3.6	>100	>100
2	22.2 ± 1.6	36.0 ± 3.1	93.4 ± 2.2	46.2 ± 2.1	52.2 ± 2.7	>100	>100
3	6.2 ± 0.5	14.0 ± 1.2	54.6 ± 3.9	21.6 ± 1.8	>100	69.1 ± 4.3	68.4 ± 3.5
Cisplatin	3.4 ± 0.4	11.4 ± 0.5	12.6 ± 1.5	13.3 ± 2.0	–	6.8 ± 1.1	9.3 ± 1.3

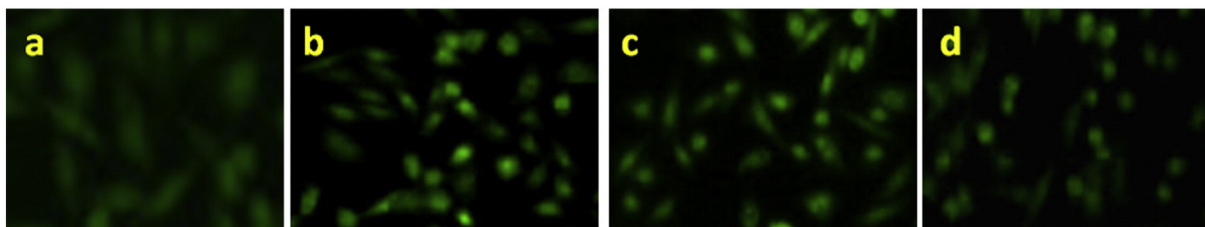


Fig. 1. Apoptosis in SGC-7901 cells (a), exposure to 6.25 μM of complexes **1** (b), **2** (c), and **3** (d) for 24 h and the cells were stained with AO/EB.

2.5. The percentage of apoptotic cells determination by flow cytometry

After chemical treatment, 1×10^6 cells were harvested, washed with PBS, fixed with 70% ethanol, and finally maintained at 4 $^{\circ}\text{C}$ for at least 24 h. The pellets were stained with a fluorescent probe solution containing 50 mg/mL PI and 1 mg/mL annexin in PBS on ice in the dark for 15 min. The fluorescence emission was measured at 530 nm and 575 nm (or equivalent) using 488 nm excitation with a FACS Calibur flow cytometry (Beckman Dickinson & Co., Franklin Lakes, NJ). A minimum of 10000 cells were analyzed per sample.

2.6. Reactive oxygen species (ROS) detection

SGC-7901 cells were seeded into six-well plates (Costar, Corning Corp., New York) at a density of 2×10^5 cells per well and incubated for 24 h. The cells were cultured in RPMI 1640 supplemented with

10% of fetal bovine serum (FBS) and incubated at 37 $^{\circ}\text{C}$ and 5% CO_2 . The medium was removed and replaced with medium (final DMSO concentration, 0.05% v/v) containing complexes **1**, **2** and **3** (6.25 μM) for 24 h. The medium was removed again. The fluorescent dye 2',7'-dichlorodihydro-fluorescein diacetate ($\text{H}_2\text{DCF-DA}$) was added to the medium with a final concentration of 10 μM to cover the cells. The treated cells were then washed with cold PBS-EDTA twice, collected by trypsinization and centrifugation at 1500 rpm for 5 min, and resuspended in PBS-EDTA. Fluorescence intensity was determined by a FACSCalibur flow cytometry with an excitation wavelength of 488 nm and emission at 525 nm.

2.7. Mitochondrial membrane potential assay

SGC-7901 cells were treated for 24 h with 6.25 μM of complexes **1**, **2** and **3** in 12-well plates and were then washed three times with cold

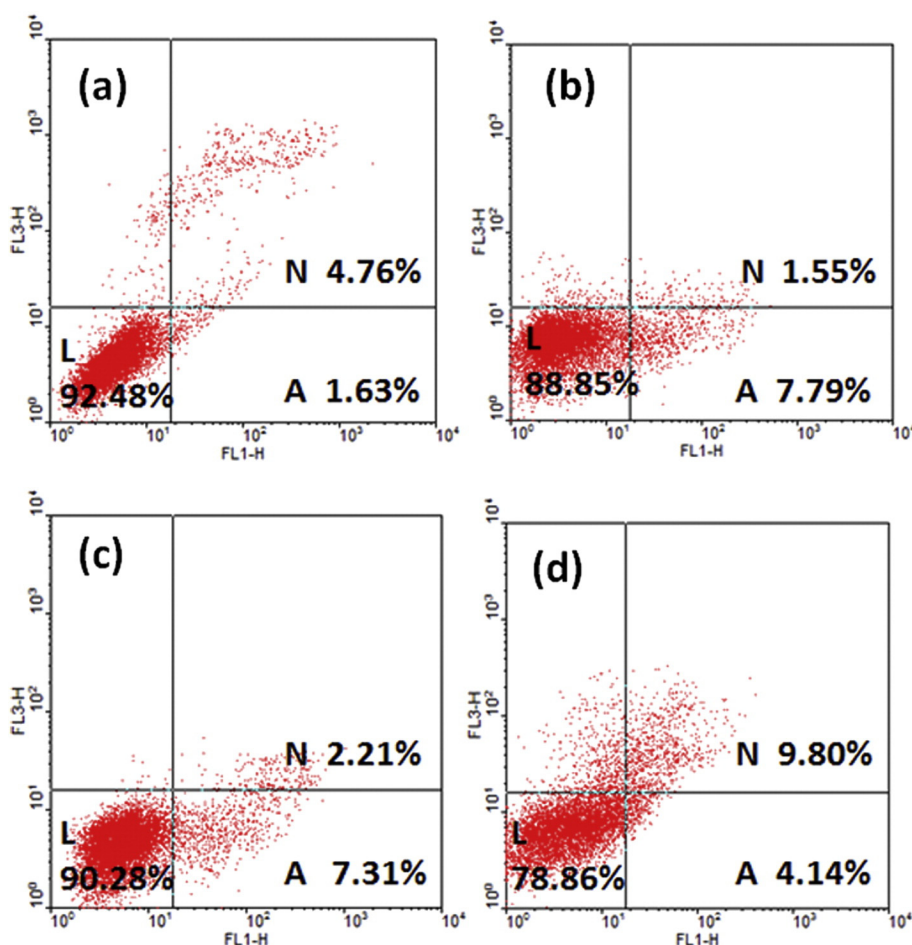


Fig. 2. The apoptotic percentage of SGC-7901 cell (a) was treated with 6.25 μM of complexes **1** (b), **2** (c), and **3** (d) for 24 h.

PBS. The cells were detached with trypsin–EDTA solution. Collected cells were incubated for 20 min with 1 mg/mL of JC-1 in culture medium at 37 °C in the dark. Cells were immediately centrifuged to remove the supernatant. Cell pellets were suspended in PBS and imaged under fluorescence microscope and the red (525 nm) and green (590 nm) fluorescent intensity was analyzed with a FACSCalibur flow cytometry.

2.8. Cell cycle arrest by flow cytometry

SGC-7901 cells were seeded into six-well plates (Costar, Corning Corp., New York) at a density of 1×10^6 cells per well and incubated for 24 h. The cells were cultured in RPMI 1640 supplemented with 10% of FBS, and incubated at 37 °C and 5% CO₂. The medium was removed and replaced with medium (final DMSO concentration 0.05% v/v) containing 6.25 μM complexes **1**, **2** and **3**. After incubation for 24 h, the cell layer was trypsinized and washed with cold phosphate buffered saline (PBS) and fixed with 70% ethanol. Twenty μL of RNase (0.2 mg/mL) and 20 μL of propidium iodide (0.02 mg/mL) were added to the cell suspensions and the mixtures were incubated at 37 °C for 30 min. The samples were then analyzed with a FACSCalibur flow cytometry. The number of cells analyzed for each sample was 10,000.

2.9. Anti-metastasis study

The BD BioCoat™ Matrigel™ invasion chamber (BD Biosciences) was used according to the manufacturer's instructions. Compounds were dissolved in cell media at the desired concentration and dissolved in Matrigel. Twenty-five thousands of SGC-7901 cells in serum free media were then seeded in the top chamber of the two chamber

Matrigel system. To the lower compartment, RPMI and 5% FBS were added as chemo-attractant. Cells were allowed to invade for 24 h. After incubation, non-invading cells were removed from the upper surface and cells on the lower surface were fixed and stained with Diff-Quik kit (BD Biosciences). Membranes were photographed and the invading cells were counted under a light microscope. Mean values from three independent assays were calculated.

2.10. Western blot analysis

SGC-7901 cells were seeded in 3.5 cm dishes for 24 h and incubated with complexes **1**, **2**, and **3** with the concentration of 6.25 μM in the presence of 10% FBS. Then cells were harvested in lysis buffer. After sonication, the samples were centrifuged for 20 min at 13,000 g. The protein concentration of the supernatant was determined by BCA assay. Sodium dodecyl sulfate–polyacrylamide gel electrophoresis was done loading equal amount of proteins per lane. Gels were then transferred to poly(vinylidene difluoride) membranes (Millipore) and blocked with 5% non-fat milk in TBST buffer for 1 h. Then the membranes were incubated with primary antibodies at 1:3000 dilutions TBST overnight at 37 °C, and washed four times with TBST for a total of 30 min. After which the secondary antibodies conjugated with horseradish peroxidase at 1:3000 dilution for 1 h at room temperature and then washed four times with TBST. The blots were visualized with the Amersham ECL Plus Western blotting detection reagents according to the manufacturer's instructions. To assess the presence of comparable amount of proteins in each lane, the membranes were stripped finally to detect the GAPDH.

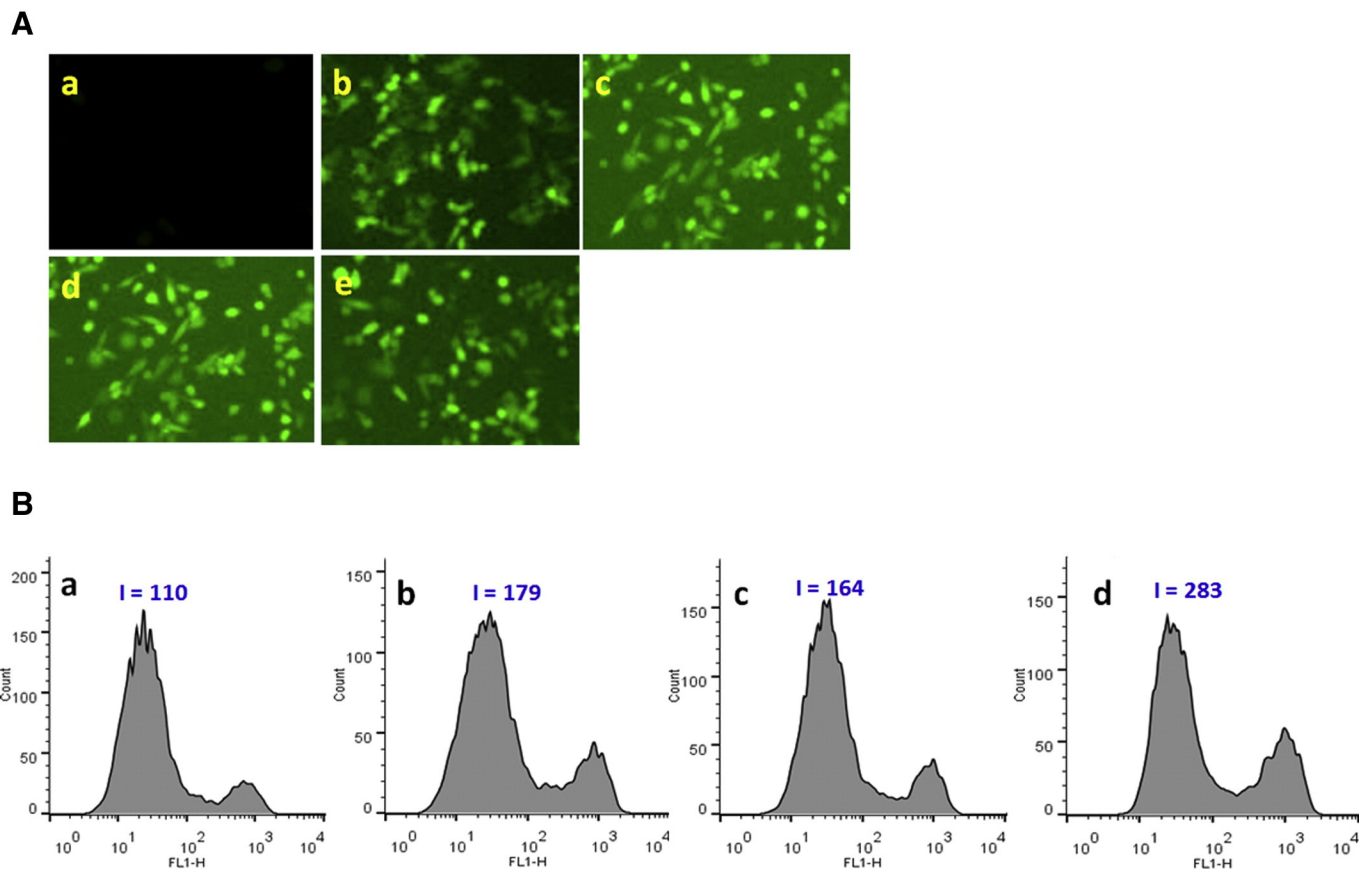


Fig. 3. (A) Intracellular ROS was detected in SGC-7901 cells (a) exposure to Rosup (positive control, b) and 6.25 μM of complexes **1** (c), **2** (d) and **3** (e) for 24 h. (B) The DCF fluorescent intensity in SGC-7901 cells (a) induced by **1** (b), **2** (c) and **3** (d) for 24 h was determined by flow cytometry.

3. Results and discussion

3.1. Synthesis and characterization

The ligand TCPI was prepared by 2-(3-aminophenyl)imidazo[4,5-*f*][1,10]phenanthroline and 1,8-naphthalic anhydride in DMF. The complexes were synthesized by the reaction of refluxing relative precursor with TCPI in ethanol. The synthesized complexes were characterized by ES-MS, ^1H NMR and elemental analysis. In the IR spectra assay (Fig. S1, supporting information), the peaks of 3543.5 cm^{-1} for TCPI, 3627.2 cm^{-1} for **1**, 3495.5 cm^{-1} for **2** and 3645.8 cm^{-1} for **3** are assigned to N–H stretching vibration. The peaks of 3066.3 cm^{-1} for TCPI, 3071.3 cm^{-1} for **1**, 3064.9 cm^{-1} for **2**, 3066.3 cm^{-1} for **3** are attributed to the C–H stretching vibration. Moreover, the peaks of 1704.9 cm^{-1} for TCPI, 1708.0 cm^{-1} for **1**, 1708.5 cm^{-1} for **2** and 1708.6 cm^{-1} for **3** demonstrate the existence of carbonyl group. In the ES-MS spectra for the Ru(II) complexes, all of the expected signals $[\text{M}-\text{PF}_6]^+$, $[\text{M}-2\text{PF}_6-\text{H}]^+$ and $[\text{M}-2\text{PF}_6]^2+$ were observed. The measured molecular weights were consistent with the expected values (Fig. S2, supporting information). As shown in Fig. S3 (supporting information), the absorption spectra of complexes **1–3** mainly consist of two or three resolved bands in the range of 200–600 nm. The bands below 300 nm are attributed to intraligand (IL) $\pi \rightarrow \pi^*$ transitions and the lowest energy bands at 458 nm for complex **1**, 454 nm for **2** and 470 nm for **3** are assigned to the metal-to-ligand charge transfer (MLCT) transitions. The complexes **1** and **2** can emit luminescence in PBS solution at ambient temperature,

with a maximum appearing at 589 nm and 586 nm, respectively. The complex **3** emits weak luminescence in PBS solution (Fig. S4, supporting information). These data indicate that the ligand and its three complexes have been synthesized.

3.2. Cytotoxic activity in vitro

The complexes **1–3** against SGC-7901, PC-12, HepG-2, SiHa, Eca-109, HeLa, and normal cell line LO2 were evaluated using MTT assays, and cisplatin was used as a reference. The selected cells were treated with the different concentrations of the complexes **1–3** for 48 h, and then the cell viability was detected. The IC_{50} values are listed in Table 1, all the complexes can effectively inhibit the proliferation of SGC-7901 and PC-12 cells. The complexes **1–3** show relatively low cytotoxic activity against HepG-2 and SiHa cells. However, complex **3** displays the highest cytotoxicity against SGC-7901, PC-12, HepG-2, SiHa and HeLa cells among the complexes. This may be caused by larger hydrophobicity of ancillary dmp than those of bpy and phen. Surprisingly, complexes **1–3** have no cytotoxicity or low cytotoxic activity against normal cell LO2. This is less observed in the studies of ruthenium(II) polypyridyl complexes on the anticancer activity. From the data, we can easily conclude that all the complexes demonstrate different cytotoxicities toward different cell lines and the same complex exhibits different inhibitory effects on the cell growth toward different cancer cells. Comparing the IC_{50} values, the complexes show lower cytotoxicity than cisplatin against the selected cancer cell lines under identical conditions.

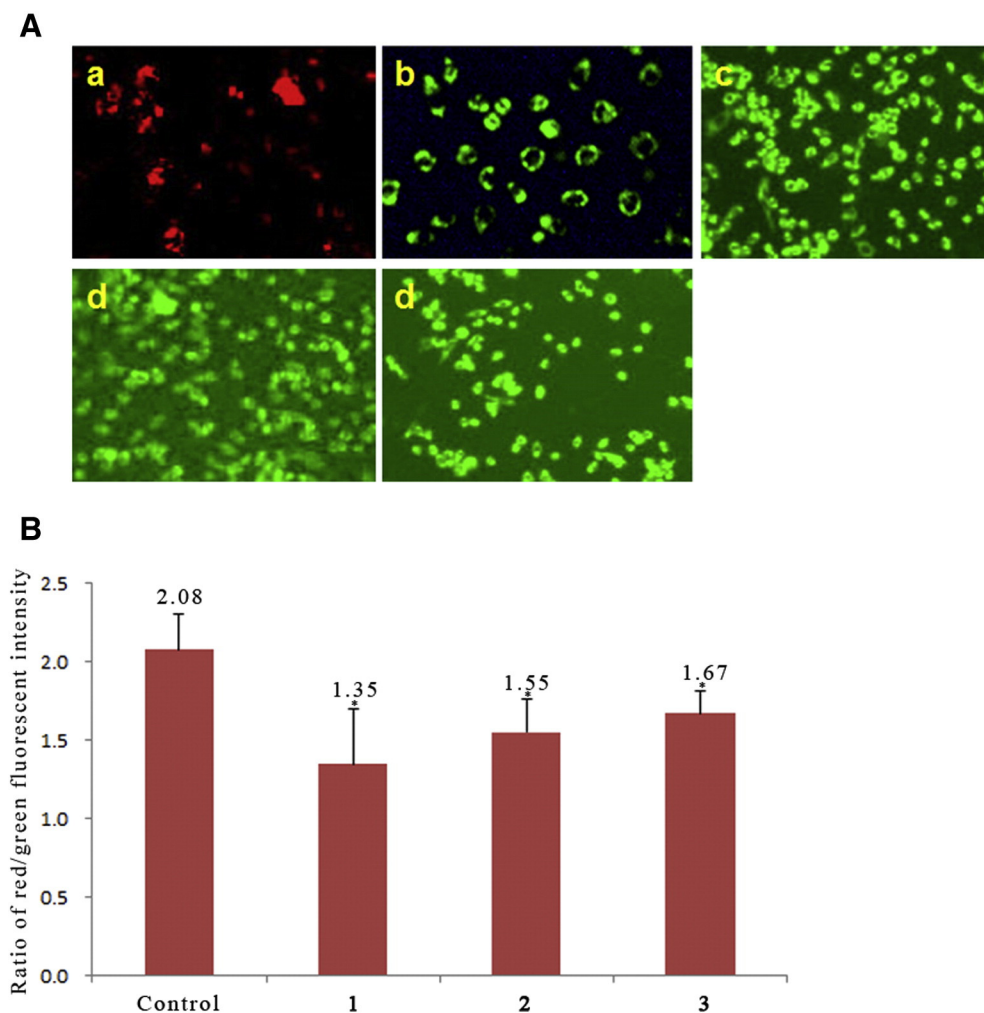


Fig. 4. (A) Assay of SGC-7901 cells mitochondrial membrane potential with JC-1 as fluorescent probe. SGC-7901 cells (a) exposed to cccp (positive control, b) and 6.25 μM of complexes **1** (c), **2** (d) and **3** (e) for 24 h. (B) The ratio of red/green fluorescence was determined by flow cytometry. SGC-7901 cells exposure to 6.25 μM of complexes **1–3** for 24 h.

Comparing with other ruthenium(II) complexes, the cytotoxicity of the complexes is lower than those of $[\text{Ru}(\text{phen})_5\text{-idip}]^{2+}$ ($\text{IC}_{50} = 34.6 \pm 1.7 \mu\text{M}$) [35] and $[\text{Ru}(\text{phen})_2(\text{DHBT})]^{2+}$ ($\text{IC}_{50} = 30.1 \pm 2.7 \mu\text{M}$) [36] against HepG2 cell. Because SGC-7901 cells are sensitive to the complexes, this cell line was selected for further experiments.

3.3. Apoptosis assay by AO/EB staining method

According to the features of cell morphology and cell membrane integrity, necrotic and apoptotic cells can be distinguished under fluorescence microscope. In order to assess whether complexes **1–3** can cause apoptosis in SGC-7901 cells, the apoptosis was investigated with acridine orange (AO) and ethidium bromide (EB) staining method. As shown in Fig. 1, in control (a), the living cells exhibited brightly green fluorescence. However, SGC-7901 cells were treated with $6.25 \mu\text{M}$ of complexes **1** (b), **2** (c) and **3** (d) for 24 h, the cells had the typical apoptotic features including cell blebbing, nuclear shrinkage and chromatin condensation. These characteristics suggest that the complexes can induce apoptosis in SGC-7901 cells. To quantitatively compare the effect of the complexes on apoptosis, the apoptosis was also assayed with flow cytometry. As shown in Fig. 2, in control (a), the percentage in apoptotic cells is 1.63%. After the treatment of SGC-7901 cell with $6.25 \mu\text{M}$ of complexes **1** (b), **2** (c) and **3** (d) for 24 h, the percentages in the apoptotic cells are 7.79%, 7.31% and 4.14%, respectively. The apoptotic effect follows the order of **1** > **2** > **3**, which is not consistent with that of cytotoxicity of the complexes against SGC-7901 cell. In other words, it is possible that the complex with high cytotoxic activity shows low apoptotic effect.

3.4. Reactive oxygen species (ROS) detection

ROS plays a crucial role in mediating apoptosis of cells [37]. In order to elucidate whether the complexes can increase the ROS levels, ROS levels were detected with $\text{H}_2\text{DCF-DA}$ (2',7'-dichlorodihydrofluorescein diacetate) as fluorescent probe. $\text{H}_2\text{DCF-DA}$ is a cell permeant dye that can cross the cell membrane freely and can be hydrolyzed by intracellular esterases into DCFH. Then DCFH is oxidized by intracellular free radicals to DCF (dichlorofluorescein), DCF can emit fluorescence [38,39]. As shown in Fig. 3A, in control (a), no fluorescent spots are found. After the treatment of SGC-7901 cell with Rosup (b, positive control) and $6.25 \mu\text{M}$ of complexes **1** (c), **2** (d) and **3** (e) for 24 h, a number of bright green fluorescent spots are observed. The results indicate that the complexes can enhance the ROS levels. To quantitatively compare the effect of the complexes on ROS levels, the DCF fluorescent intensity was determined by flow cytometry. In the control (Fig. 3B (b)), the DCF fluorescent intensity is 110, SGC-7901 cells were exposed to $6.25 \mu\text{M}$ of complexes **1** (b), **2** (c) and **3** (d) for 24 h, the DCF fluorescent intensity is 179, 164 and 283, respectively. Obviously, the fluorescent intensity of DCF increases 1.63, 1.49 and 2.57 times than that of the original. Complex **3** shows greater effect on the ROS levels than complexes **1** and **2** under the same conditions.

3.5. Mitochondrial membrane potential assay

Apoptosis or programmed cell death can be activated through two main pathways, namely, death receptor-mediated apoptosis (extrinsic pathway) and mitochondria-mediated apoptosis (intrinsic pathway)

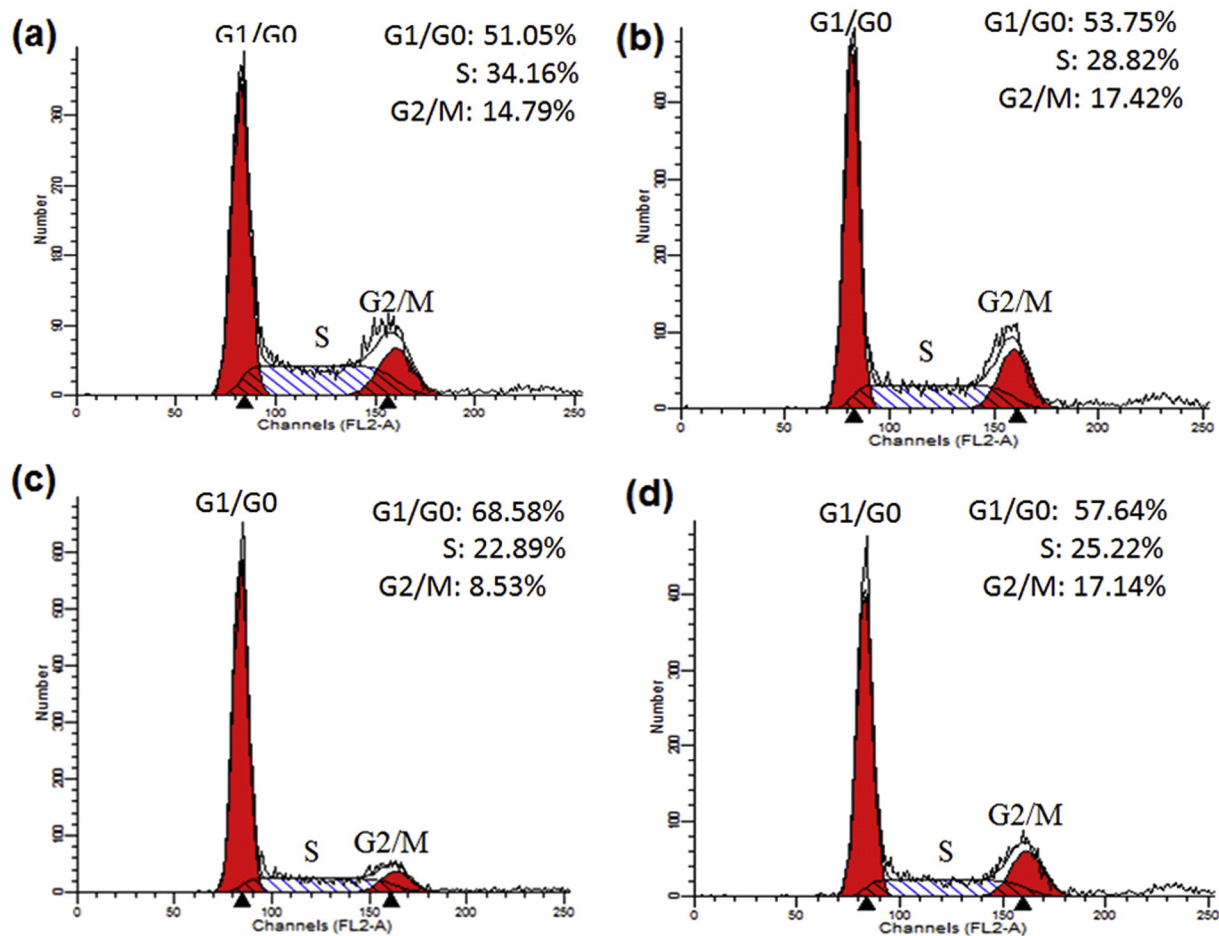


Fig. 5

Fig. 5. Cell cycle arrest of SGC-7901 cells (a) exposure to $6.25 \mu\text{M}$ of complexes **1** (b), **2** (c) and **3** (d) for 24 h.

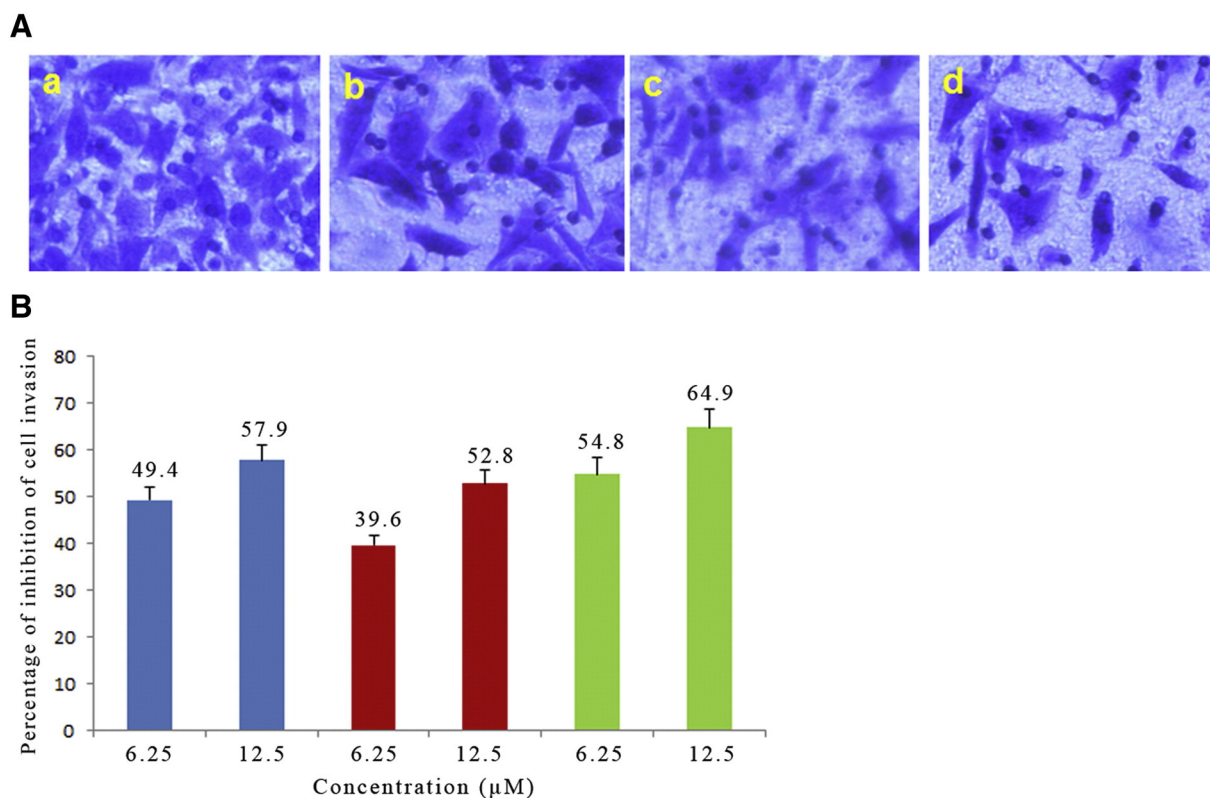


Fig. 6. (A) Microscope images of invading SGC-7901 cells that have migrated through the Matrigel: The extent of inhibition of cell invasion by complexes **1** (b), **2** (c) and **3** (d) against SGC-7901 (a) cells can be seen from the decrease in the numbers of invading cells. (B) The percentage of inhibition cell invasion induced by different concentrations of complexes **1** (blue), **2** (red) and **3** (green) for 24 h. (For interpretation of the references to colour in this figure legend, the reader is referred to the web version of this article.)

[40]. Mitochondria have emerged as a point of integration for apoptotic signals originating from both the extrinsic and intrinsic apoptotic pathways [41,42]. It is well known that the mitochondria membrane potential (MMP, $\Delta\Psi_m$) is a major event in the early apoptosis, and JC-1 was used as fluorescent probe to assess the changes in $\Delta\Psi_m$ [43–45]. When the mitochondrial membrane potential is high, JC-1 accumulates in matrix to constitute JC-1 aggregates that can emit red fluorescence. On the contrary, JC-1 forms monomer and emits green fluorescence corresponding to low mitochondrial membrane potential. As shown in Fig. 4A, in control (a), bright red fluorescence was found. After the SGC-7901 cells were exposed to cccp (b, positive control) and 6.25 μM of complexes **1** (c), **2** (d) and **3** (e) for 24 h, JC-1 emits green fluorescence. The changes from red to green demonstrate that the reduction of mitochondrial membrane potential occurred. To quantitatively compare the changes of MMP induced by the complexes, the ratio of the red and green fluorescent intensity was detected using flow cytometry. As illustrated in Fig. 4B, in the control, the ratio of red/green is 2.08. After SGC-7901 cells were treated with 6.25 μM of the complexes **1–3** for 24 h, the ratios of red/green are 1.35, 1.55 and 1.67, respectively. Complex **1** reveals the most effective on the changes of mitochondrial membrane potential. The results indicate that the complexes can induce a decrease in the mitochondrial membrane potential and follows the order of **1** > **2** > **3**.

3.6. Cell cycle arrest by flow cytometry

The cell cycle plays a key role in the regulation of cells. The cell cycle distribution was investigated by flow cytometry. As shown in Fig. 5, in control (a), the percentage in the cell at G0/G1 is 51.05%. After SGC-7901 cells were treated with 6.25 μM of complexes **1** (b), **2** (c) and **3** (d) for 24 h, the percentages in the cell at G0/G1 are 53.75%, 68.58% and 57.64%, respectively. An increase of 3.70%, 17.53% and 6.59% for complexes **1–3** is observed, accompanied corresponding to reduction

in the percentage of cell at S phase. These results demonstrate that complexes **1**, **2** and **3** induce cell cycle arrest at G0/G1 phase in SGC-7901 cells.

3.7. Anti-metastasis studies

Cell invasion is a process which is typically associated with cancer cell metastasis, and it refers to three dimensional migration of cells as they penetrate an extracellular matrix (ECM) [46]. Complexes play a role in anti-metastatic because they lead to a decrease of the amount

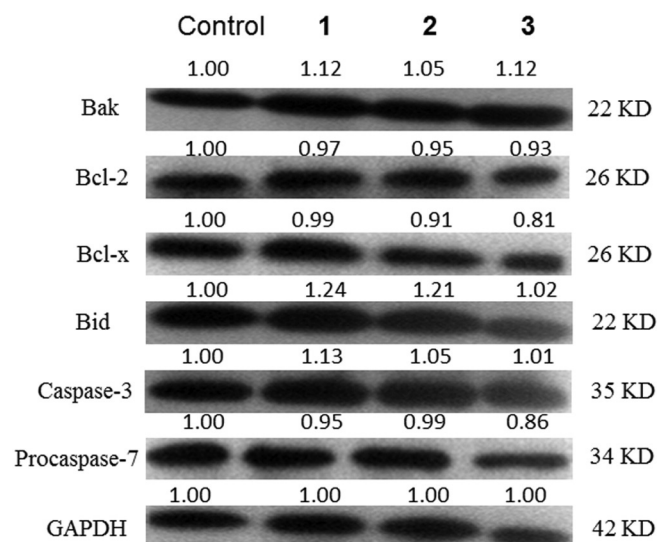


Fig. 7. SGC-7901 cells were treated with 6.25 μM of the complexes for 24 h and the expression levels of the apoptosis-related proteins were examined by Western blot.

of viable cells which traverse through the Matrigel compared with the control. To determine the efficiency of complexes **1–3** inhibiting the cell invasion, the Matrigel invasion assay was performed. The results are shown in Fig. 6A and B. After SGC-7901 cells were exposed to 12.5 μM of complexes **1–3**, the percentage of inhibiting the cell invasion is 57.9%, 52.8% and 64.9%, respectively. Therefore, complex **3** shows greater anti-invasive activity than complexes **1** and **2** under identical conditions. Moreover, complexes **1–3** inhibit the invasion of SGC-7901 cells in a concentration-dependent manner.

3.8. Western blot analysis

Apoptosis is a cellular death mechanism that many different genes are involved in its regulation. In general, caspases which are a family of cysteine proteases have been paid particular attention as they play essential roles in necrosis, inflammation, and apoptosis [47]. Among them, caspase-3 and caspase-7 are considered as activators of apoptosis in extrinsic and intrinsic apoptosis pathways [48]. Bcl-2 family proteins and caspases play a key role in regulating apoptosis. The effects of the complexes on the expression of caspases and Bcl-2 family proteins were assayed by Western blot. As illustrated in Fig. 7, treatment of SGC-7901 cells with complexes **1–3** resulted in an increase in the expression of Bak, Bid and caspase-3, whereas the expression in the levels of Bcl-2, Bcl-x and procaspase-7 downregulated. Thus, the complexes can regulate the expression of Bcl-2 family proteins.

4. Conclusions

We synthesized three new ruthenium(II) complexes and evaluated their *in vivo* anticancer activities. The cytotoxicity *in vitro* assay indicates that complexes **1–3** show good potential for inhibiting cell proliferation in SGC-7901. Different complexes show different cytotoxicity against the selected cell lines. The complexes can effectively induce SGC-7901 cells apoptosis. Complexes **1–3** can lead to an enhancement in ROS levels and induce a reduction in mitochondrial membrane potential. The results from the cell cycle arrest displayed that complexes induce cell cycle arrest in SGC-7901 cells at G0/G1 phase. The complexes can inhibit the cell invasion; the complexes at 12.5 μM show to be more effective in inhibiting cell invasion than those at 6.25 μM . In addition, the complexes can regulate the expression of Bcl-2 family proteins and caspase 3 and procaspase 7. In conclusion, the complexes induce apoptosis in SGC-7901 cell through a ROS-mediated mitochondrial dysfunction pathway, which was accompanied by the regulation of the expression of Bcl-2 family proteins. This work will be helpful for designing and synthesizing new ruthenium complexes as potential anticancer drugs.

Acknowledgments

This work was supported by the Natural Science Foundation of Guangdong Province (Nos. 2016A030313726, 2016A030313728), the High-Level Personnel Project of Guangdong Province in 2013 and the Joint Nature Science Fund of the Department of Science and Technology and the First Affiliated Hospital of Guangdong Pharmaceutical University (No GYFYLH201315).

Appendix A. Supplementary material

Supplementary data to this article can be found online at <http://dx.doi.org/10.1016/j.inoche.2016.06.020>.

References

- [1] M.A. Fuertes, C. Alonso, J.M. Perez, *Chem. Rev.* 103 (2003) 645.
- [2] Y. Jung, S.J. Lippard, *Chem. Rev.* 107 (2007) 1387.
- [3] T. Boulikas, M. Vougiouka, *Oncol. Rep.* 10 (2003) 1663.
- [4] E. Wong, C.M. Giandomenico, *Chem. Rev.* 99 (1999) 2451.
- [5] E.R. Jamieson, S.J. Lippard, *Chem. Rev.* 99 (1999) 2467.
- [6] I. Kostova, *Recent Pat. Anticancer Drug Discov.* 1 (2006) 1.
- [7] S. Medici, M. Peana, V.M. Nurchi, J.I. Lachowicz, G. Crisponi, M.A. Zoroddu, *Coord. Chem. Rev.* 284 (2015) 329.
- [8] C. Qian, J.Q. Wang, C.L. Song, L.L. Wang, L.N. Ji, H. Chao, *Metalomics* 5 (2013) 844.
- [9] A.L. Noffke, A. Habtemarian, A.M. Pizarro, P.J. Sadler, *Chem. Commun.* 48 (2012) 5219–5246.
- [10] S. Komeda, A. Casini, *Curr. Top. Med. Chem.* 12 (2012) 219.
- [11] J.Q. Wang, P.Y. Zhang, C. Qian, X.J. Hou, L.N. Ji, H. Chao, *J. Biol. Inorg. Chem.* 19 (2014) 335.
- [12] A. Bergamo, G. Sava, *Dalton Trans.* 40 (2011) 7817.
- [13] A. Bergamo, C. Gaiddon, J.H. Schellens, J.H. Beijnen, G. Sava, *J. Inorg. Biochem.* 106 (2012) 90.
- [14] P. Heffeter, K. Bock, B. Atil, M.A.R. Hoda, W. Korner, C. Bartel, U. Jungwirth, B.K. Keppler, M. Micksche, W. Berger, G. Koellensperger, *J. Biol. Inorg. Chem.* 15 (2010) 737.
- [15] M. Groessl, O. Zava, P.J. Dyson, *Metalomics* 3 (2011) 591.
- [16] R. Trondl, P. Heffeter, C.R. Kowol, M.A. Jakupec, W. Berger, B.K. Keppler, *Chem. Sci.* 5 (2014) 2925.
- [17] C.G. Hartinger, M.A. Jakupec, S. Zorbas-Seifried, M. Groessl, A. Egger, W. Berger, H. Zorbas, P.J. Dyson, B.K. Keppler, *Chem. Biodivers.* 5 (2008) 2140.
- [18] C.G. Hartinger, S. Zorbas-Seifried, M.A. Jakupec, B. Kynast, H. Zorbas, B.K. Keppler, *J. Inorg. Biochem.* 100 (2006) 891.
- [19] T. Gianferrara, I. Bratsos, E. Alessio, *Dalton Trans.* 37 (2009) 7588.
- [20] S.H. Lai, G.B. Jiang, J.H. Yao, W. Li, B.J. Han, C. Zhang, C.C. Zeng, Y.J. Liu, *J. Inorg. Biochem.* 152 (2015) 1.
- [21] B. Peña, A. David, C. Pavan, M.S. Baptista, J.P. Pellois, C. Turro, K.M. Dunbar, *Organometallics* 33 (2014) 1100.
- [22] H.Y. Huang, P.Y. Zhang, B.L. Yu, Y.J. Chen, Q. Wang, L.N. Ji, H. Chao, *J. Med. Chem.* 57 (2014) 8971.
- [23] U. Schatzschneider, J. Niesel, I. Ott, R. Gust, H. Alborzina, S. Wolf, *ChemMedChem* 3 (2008) 1104.
- [24] V. Pierroz, T. Joshi, A. Leonidova, C. Mari, J. Schur, I. Ott, L. Spiccia, S. Ferrari, G. Gasser, *J. Am. Chem. Soc.* 134 (2012) 20376.
- [25] M.J. Pisani, P.D. Fromm, Y. Mulyana, R.J. Clarke, H. Korner, K. Heimann, J.G. Collins, F.R. Keene, *ChemMedChem* 6 (2011) 848.
- [26] W. Li, B.J. Han, J.H. Yao, G.B. Jiang, Y.J. Liu, *RSC Adv.* 5 (2015) 24534.
- [27] G.B. Jiang, X. Zheng, J.H. Yao, B.J. Han, W. Li, J. Wang, H.H. Liang, Y.J. Liu, *J. Inorg. Biochem.* 141 (2014) 170.
- [28] T.F. Chen, Y.N. Liu, W.J. Zheng, J. Liu, Y.S. Wong, *Inorg. Chem.* 49 (2010) 6366.
- [29] G.J. Lin, G.B. Jiang, Y.Y. Xie, H.L. Huang, Z.H. Liang, Y.J. Liu, *J. Biol. Inorg. Chem.* 18 (2013) 873.
- [30] X.X. Yang, L.M. Chen, Y.N. Liu, Y.G. Yang, T.F. Chen, W.J. Zheng, J. Liu, Q.Y. He, *Biochimie* 94 (2012) 345.
- [31] H.L. Huang, Y.J. Liu, C.H. Zeng, L.X. He, F.H. Wu, *DNA Cell Biol.* 29 (2010) 261.
- [32] B.P. Sullivan, D.J. Salmon, T.J. Meyer, *Inorg. Chem.* 17 (1978) 3334.
- [33] J.P. Collin, J.P. Sauvage, *Inorg. Chem.* 25 (1986) 135.
- [34] T. Mosmann, *J. Immunol. Methods* 65 (1983) 55.
- [35] Q.Q. Yu, Y.N. Liu, L. Xu, C.P. Zheng, F.L. Le, X.Y. Qin, Y.Y. Liu, J. Liu, *Eur. J. Med. Chem.* 82 (2014) 82–95.
- [36] W. Li, B.J. Han, J.H. Yao, G.B. Jiang, Y.J. Liu, *RSC Adv.* 5 (2015) 24534–24543.
- [37] J.L. Martindale, N.J. Holbrook, *J. Cell. Physiol.* 192 (2002) 1.
- [38] L.R. Silveira, L. Pereira-Da-Silva, C. Juel, Y. Hellsten, *Free Radic. Biol. Med.* 35 (2003) 455.
- [39] K. Ito, A. Hirao, F. Arai, K. Takubo, S. Matsuoka, K. Miyamoto, M. Ohmura, K. Naka, K. Hosokawa, Y. Ikeda, T. Suda, *Nat. Med.* 12 (1997) 446.
- [40] N.A. Thornberry, T.A. Rano, E.P. Peterson, D.M. Rasper, T. Timkey, M. Garcia-Calvo, V.M. Houtzager, P.A. Nordstrom, S. Roy, J.P. Vaillancourt, K.T. Chapman, D.W. Nicholson, *J. Biol. Chem.* 272 (1997) 17907.
- [41] T. Chen, Y.S. Wong, *Int. J. Biochem. Cell Biol.* 41 (2009) 666.
- [42] T. Chen, Y.S. Wong, *Cell. Mol. Life Sci.* 65 (2008) 2763.
- [43] L. Wang, K.Y. Lu, H.H. Hao, X.Y. Li, J. Wang, K. Wang, J. Wang, Z. Yan, S.L. Zhang, Y.H. Du, H.R. Liu, *PLoS One* 8 (2013), e81296.
- [44] E. Cavaliere, A. Rigo, M. Bonifacio, A.C.D. Prati, E. Guardalben, C. Bergamini, R. Fato, G. Pizzolo, H. Suzuki, F. Vinante, *J. Transl. Med.* 9 (2011) 45.
- [45] Y.S. Shin, H.A. Shin, S.U. Kang, J.H. Kim, Y.T. Oh, K.H. Park, C.H. Kim, *PLoS One* 8 (2013), e6915.
- [46] R. Horwitz, D. Webb, *Curr. Biol.* 13 (2003) R756.
- [47] G.S. Salvesen, S.J. Riedl, *Adv. Exp. Med. Biol.* 615 (2008) 13.
- [48] J.M. Adams, *Genes Dev.* 17 (2003) 2481.